Polar Geosci., **17**, 88–111, 2004

Occurrences of metamorphosed ultramafic rock and associating rocks in Howard Hills, Enderby Land, East Antarctica: Evidence of partial melting from geochemical and isotopic characteristics

Tomoharu Miyamoto[1]*, Yasutaka Yoshimura[2], Kei Sato[3], Yoichi Motoyoshi[4], Daniel J. Dunkley[4] and Christopher J. Carson[5†]

[1] *Department of Earth and Planetary Sciences, Kyushu University, Hakozaki, Fukuoka 812-8581*
[2] *Department of Natural Environmental Science, Kochi University, Akebono-cho, Kochi 780-8520*
[3] *Division of Earth Sciences, Department of Biosphere-Geosphere Sciences, Ehime University, Bunkyo-cho, Matsuyama 790-8577*
[4] *National Institute of Polar Research, Kaga 1-chome, Itabashi-ku, Tokyo 173-8515*
[5] *Geological Survey of Canada, 601 Booth Street, Ottawa, Ont., Canada K1A 0E8*
[†] *now at Northern Territory Geological Survey, GPO 3000, Darwin NT, 0801, Australia*
[*] *Corresponding author. E-mail: miyamoto@geo.kyushu-u.ac.jp*

(Received February 23, 2004; Accepted May 11, 2004)

Abstract: Large blocks of metamorphic rocks with mafic to ultramafic compositions were discovered in felsic gneiss at the central part of northern Howard Hills in Enderby Land. The ultramafic core is separated from the felsic gneiss by a mantle of pyroxene granulite. We can recognize from mineral assemblages and chemical compositions that the metamorphic rocks experienced ultrahigh temperature (UHT) metamorphism. Rubidium-strontium and samarium-neodymium analytical data from the metamorphic rocks yield apparent ages of about 2.65 Ga within analytical error on isochron diagrams. Metamorphic rocks with mafic to ultramafic compositions are enriched in incompatible elements and have high Sr isotope ratios, resulting in some samples in improbable Nd model ages. This is attributed to enrichment of compatible elements and/or depletion of incompatible elements during metamorphism. We conclude that these metamorphic rocks experienced partial melting during UHT metamorphism. Pyroxene granulite was produced as a residual material after partial melting of LILE-enriched protoliths with high Sr isotope ratios.

key words: Howard Hills, Napier Complex, Sr-Nd isotope chemistry, partial melting

1. Introduction

The Napier Complex of Enderby Land, East Antarctica is an Archean granulite-facies metamorphic terrane. Since 1996, the Japanese Antarctic Research Expedition (JARE) has been carrying out the "SEAL" (Structure and Evolution of east Antarctic Lithosphere) project, which is an investigation of the geology of the Napier Complex in Enderby Land with the overall aim of understanding the crustal evolution of the Precambrian shield of East Antarctica. For this purpose, field parties of JARE-38 and -39 carried out detailed geological surveys of Mount Riiser-Larsen and Tonagh Island (Ishizuka *et al*., 1998; Osanai *et al*., 1999). Geochemical studies including

isotope chemistry for the metamorphic rocks from the Napier Complex have been conducted by previous workers (*e.g.*, Sheraton *et al*., 1987; Owada *et al*., 1994, 2000; Tainosho *et al*., 1997; Suzuki *et al*., 1999).

The Howard Hills at the east of Amundsen Bay (Fig. 1) is an outcrop surveyed geologically during JARE-40 (1998–1999). During the survey, large blocks of metamorphosed mafic to ultramafic rocks were found in felsic gneiss in the central part of northern Howard Hills. Pressure-temperature conditions for granulite formation in the Howard Hills was studied (Yoshimura *et al*., 2000); however, geochemical study with isotope chemistry has not been done previously.

Sheraton *et al*. (1987) revealed that some mafic rocks from the Napier Complex have similar geochemical features to Archean komatiitic rocks. Tainosho *et al*. (1997) interpreted the mafic gneisses as derivatives from different source materials than the felsic gneiss. The nature and origin of the mafic rocks, however, are not fully understood. Yoshimura *et al*. (2000) suggests the bulk compositions of metamorphic rocks were modified by mass transportation during partial melting at the prograde stage of metamorphism. It is important to study chemical and isotopic behavior during high-grade metamorphism to understand the evolution and maturation of continental crust. Therefore, we carried out geochemical and isotopic analysis for the metamorphic rocks, especially metamorphosed ultramafic and associated rocks from the Howard Hills, to throw some light on the dispute of the evolution of the Napier Complex.

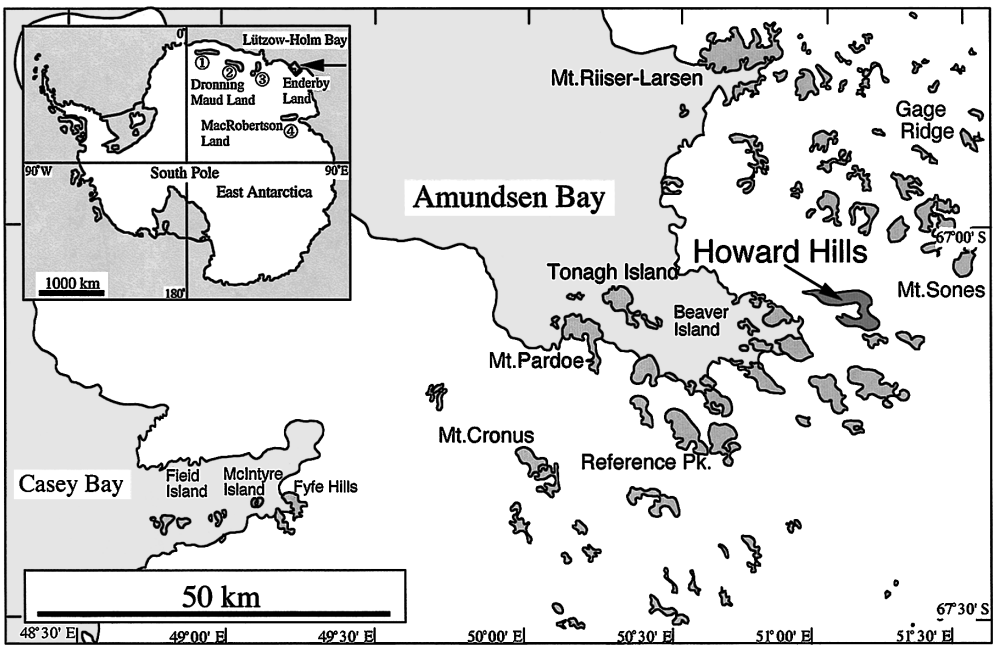

Fig. 1. Location map of Howard Hills in western Enderby Land, East Antarctica. Inset: ① Schirmacher Hills, ② Sør Rondane Mountains, ③ Yamato-Belgica Complex, and ④ Prince Charles Mountains.

2. Geological setting and petrography

The Napier Complex in East Antarctica consists of granulite-facies to UHT (ultra-high temperature) metamorphic rocks, characterized by osumilite-bearing, sapphirine-quartz and spinel-quartz mineral assemblages (Sheraton *et al*., 1987; Motoyoshi, 1998). Howard Hills (Fig. 1) is underlain by Napier Complex UHT metamorphic rocks, including garnet felsic gneiss, orthopyroxene felsic gneiss, aluminous gneiss and metamorphosed mafic to ultramafic rocks. Peak metamorphic conditions have been estimated at 1150–1200℃ (Yoshimura *et al*., 2000). Unmetamorphosed doleritic "Amundsen" dykes (Sheraton *et al*., 1987) were emplaced as NW-trending, subvertical thin sheets which crop out in the central part of the northern Howard Hills.

The area surveyed in the Howard Hills during JARE-40 is composed of layered gneisses of various origins and bulk chemistries. Garnet felsic gneiss and orthopyroxene felsic gneiss are the most abundant rock types in this area. Aluminous gneiss that is rich in garnet, sapphirine and sillimanite is present within garnet felsic gneiss as layers of variable thickness. Yoshimura *et al*. (2000) described the petrography and mineralogy of garnet felsic gneiss, aluminous gneiss and orthopyroxene felsic gneiss. Minor amounts of metamorphosed mafic to ultramafic rock are distributed sporadically as thin layers (a few tens of centimeters to meters in thickness) and as boudinaged lenticular or rounded blocks (generally a few tens of meters across). These rocks are commonly massive and medium to coarse grained.

A block of metamorphosed ultramafic rock mantled by pyroxene granulite was investigated (Fig. 2b). The rounded block is over five meters across and hosted by orthopyroxene felsic gneiss.

Orthopyroxene felsic gneiss borders pyroxene granulite (Fig. 2b), and does not contact metamorphosed ultramafic rock. Collected orthopyroxene felsic gneiss sam-

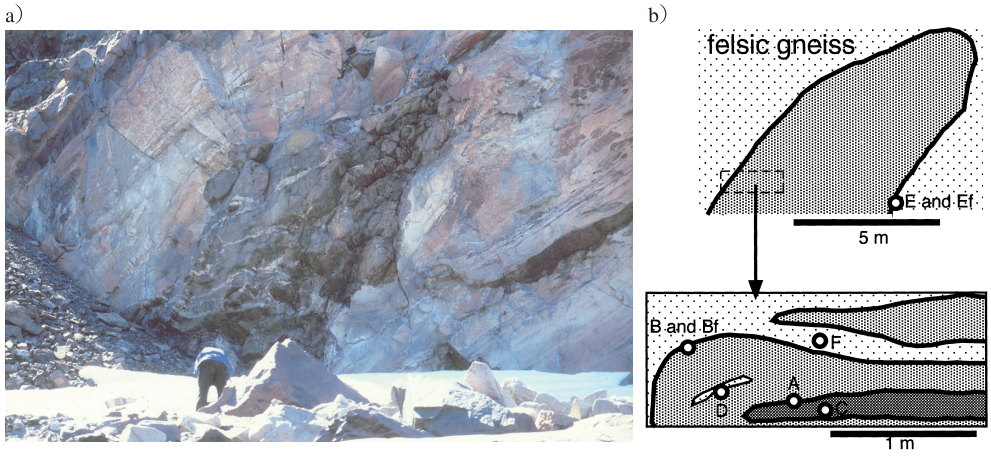

Fig. 2. (a) Investigated block of metamorphosed ultramafic rock and granulite in felsic gneiss. (b) A sketch of the block. Metamorphosed ultramafic rock constitutes a body mantled by pyroxene granulite. A–F: sampling points. Mineral assemblages of rock types are compiled in Table 1.

Table 1. Rock types and their mineral assemblages of rock samples collected from investigated mass of metamorphosed ultramafic rock and granulite in felsic gneiss.

Rock species (Sample No.)	Mineral assemblages
Metamorphosed ultramafic rock (TM981229-03C)	Ol＋Opx＋Spl＋Phl＋Serp (rare)
Pyroxene granulites	
Clinopyroxene-bearing (TM981229-03A)	Opx＋Cpx＋Pl＋Afs＋Phl (rare)
Clinopyroxene-free	
phlogopite-free (TM981229-03B, D)	Opx＋Afs＋Pl＋Qtz＋Rtl (rare)
phlogopite-bearing (TM981229-03E)	Opx＋Phl＋Spl＋Spr＋Afs＋Pl＋Ptl＋Qtz (rare)
Orthopyroxene felsic gneiss (TM981229-03Bf, Ef, F)	Opx＋Afs＋Pl＋Qtz＋Rtl＋Zrn (rare)

Afs: alkali feldspar (perthite, mesoperthite, sanidine), Cpx: clinopyroxene, Ol: olivine, Opx: orthopyroxene, Phl: phlogopite, Pl: plagioclase, Qtz: quartz, Rtl: rutile, Serp: serpentine, Spl: spinel, Spr: sapphirine, Zrn: zircon.

ples (TM981229-03Bf, Ef and F) consist of quartz, plagioclase, alkali feldspar and orthopyroxene (Fig. 3a). Alkali feldspar is perthite to mesoperthite. Rutile and zircon occur as accessory minerals in the matrix and in orthopyroxene as inclusions.

Metamorphosed ultramafic rock (TM981229-03C) is composed of dominant olivine, with subordinate orthopyroxene, spinel and phlogopite. Phlogopite is fine and colorless in thin section. Fine veins which penetrate olivine, orthopyroxene, and spinel are composed of serpentine (Fig. 3b).

Pyroxene granulite occurs between orthopyroxene felsic gneiss and metamorphosed ultramafic rock (Fig. 2b). In the granulite, small blocks of orthopyroxene felsic gneiss are observed as leucocratic portions. Pyroxene granulite is mostly composed of orthopyroxene. Orthopyroxene is coarse-grained (a few mm across) and arranged in a granoblastic polygonal texture. Only one of the pyroxene granulite samples contains subordinate clinopyroxene (TM981229-03A).

Sample TM981229-03A was taken close to the metamorphosed ultramafic rock. Subordinate clinopyroxene is pale-brown under the microscope and occurs as small grains (Fig. 3c) intergrown with coarser orthopyroxene. Orthopyroxene often contains fine clinopyroxene lamellae. Minor plagioclase, alkali feldspar and phlogopite is also present as smaller isolated grains along grain boundaries between granoblastic pyroxene.

Clinopyroxene-free pyroxene granulites occur close to the orthopyroxene felsic gneiss. One of sample contains a considerable amount of phlogopite (TM981229-03E), and others have no phlogopite (TM981229-03B and D). Phlogopite-free pyroxene granulite (TM981229-03B and D) contains subordinate quartz, plagioclase and alkali feldspar as small isolated grains along grain boundaries between orthopyroxene, and occasionally form narrow leucocratic portions (Fig. 4).

Phlogopite-bearing pyroxene granulite is composed of subsidiary alkali-feldspar, plagioclase, sapphirine and spinel, beside orthopyroxene and phlogopite (Fig. 3d). Alkali feldspar is perthite and/or sanidine. Rutile is present as a minor phase, both in orthopyroxene as acicular inclusions and along grain boundaries of orthopyroxene. Sapphirine occurs as porphyroblasts including greenish spinel, or as thin films at grain boundaries of granoblastic orthopyroxene (Fig. 3e). Mantles of blue-green sapphirine

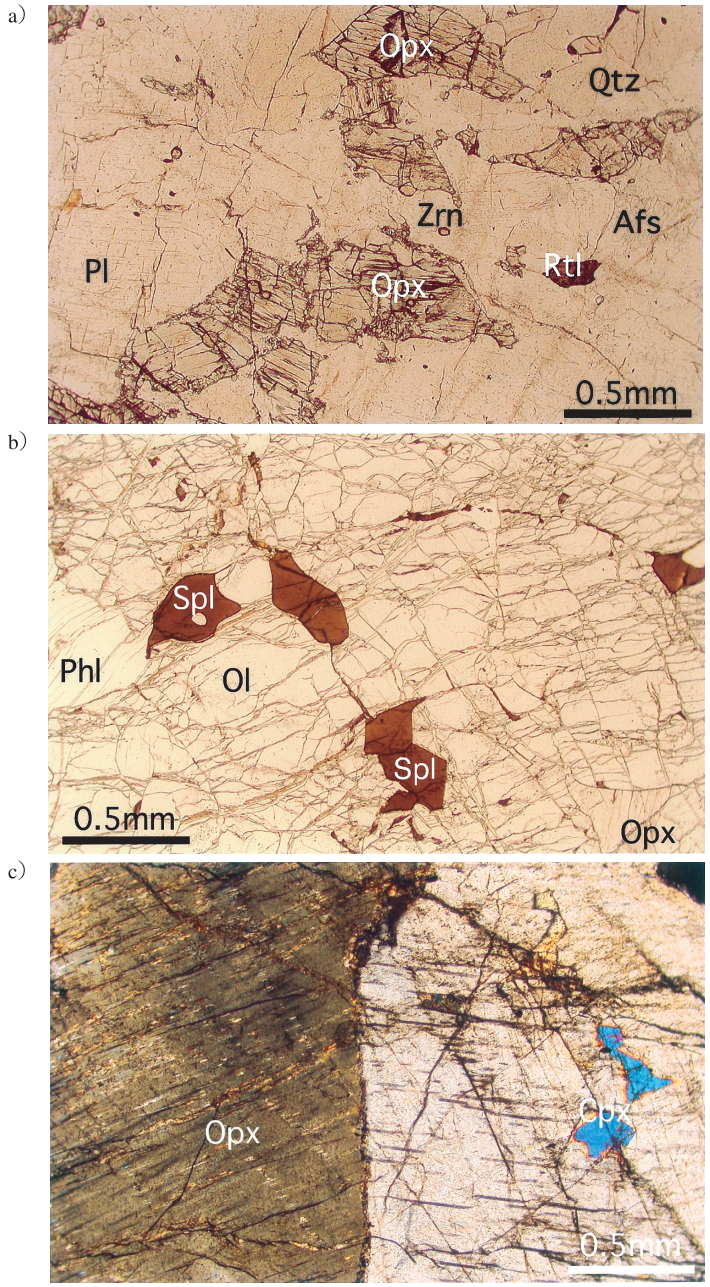

Fig. 3. (a) Orthopyroxene felsic gneiss (TM981229-03Ef). Plane-polarized light. Scale is 0.5 mm. Opx: orthopyroxene, Afs: alkali feldspar, Pl: plagioclase, Qtz: quartz, Zrn: zircon, Rtl: rutile. (b) Metamorphosed-ultramafic rock (TM981229-03C). Plane-polarized light. Scale is 0.5 mm. Ol: olivine, Opx: orthopyroxene, Spl: spinel, Phl: phlogopite. Serpentine veins penetrate olivine, orthopyroxene and spinel. (c) Clinopyroxene-bearing pyroxene granulite (TM981229-03A). Crossed polars. Scale is 0.5 mm. Opx: orthopyroxene, Cpx: clinopyroxene.

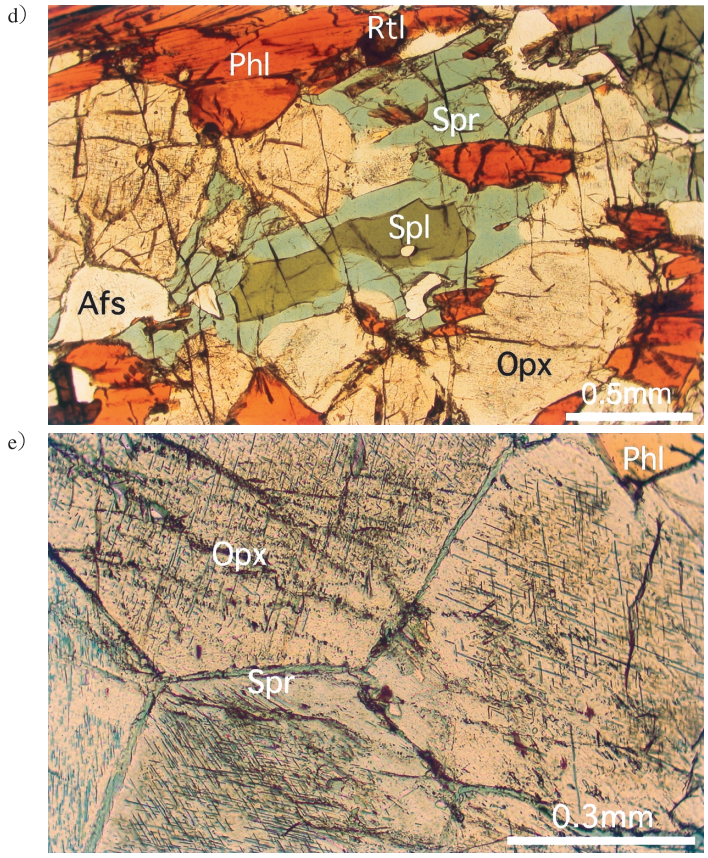

Fig. 3. (d) Pyroxene granulite with abundant phlogopite (TM981229-03E). Plane-polarized light. Scale is 0.5 mm. Opx: orthopyroxene, Afs: alkali feldspar, Phl: phlogopite, Spr: sapphirine, Spl: spinel, Rtl: rutile. (e) Pyroxene granulite with sapphirine as thin film at the grain boundaries of granoblastic orthopyroxene (TM981229-03E). Plane-polarized light. Scale is 0.3 mm. Opx: orthopyroxene, Phl: phlogopite, Spr: sapphirine. Rutile occurs as small needles in opx.

around greenish spinel are characteristic. Quartz is rare but occurs in coexistence with film-like sapphirine along grain boundaries of granoblastic orthopyroxene (Fig. 5).

3. Mineral chemistry

Chemical compositions of the major constituent minerals in metamorphosed ultramafic and associated rocks were determined using a scanning electron microscope (SEM: JEOL JSM-5800LV) with an energy dispersive X-ray analytical system (EDS: OXFORD Link ISIS) at Kyushu University. $H_2O(+)$ and $H_2O(-)$ contents of phlogopite separated from phlogopite-bearing pyroxene granulite (TM981229-03E) were determined by Karl-Fischer method (Muroi, 1979) under an N_2 atmosphere, with the temperature increased to 120°C to determine $H_2O(-)$ and then to 980°C to

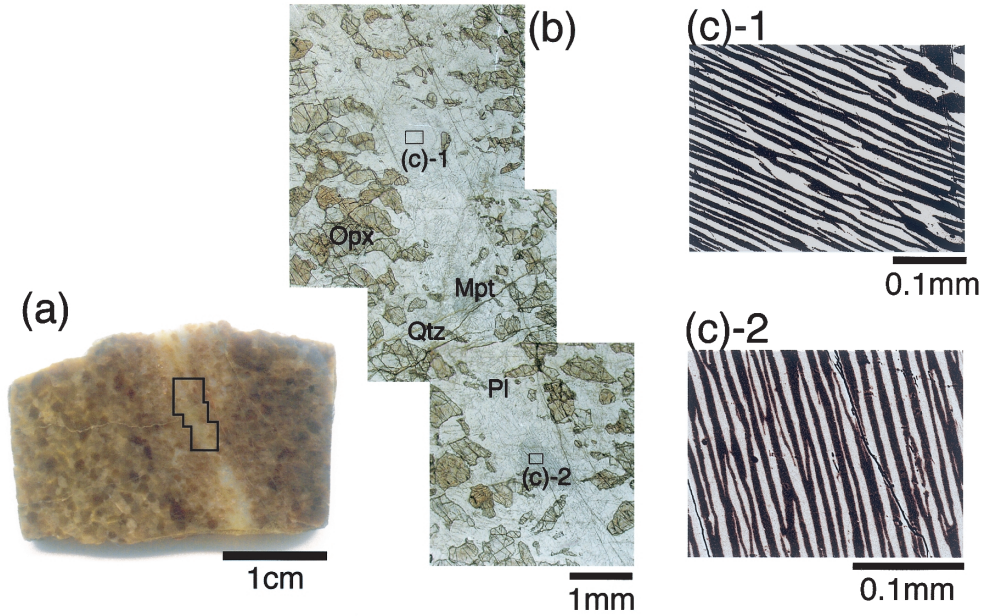

Fig. 4. Polished surface and photomicrograph of orthopyroxene granulite (TM981229-03D), and BSE image of mesoperthite in leucocratic domain on the polished surface. (a) Polished surface. (b) Photomicrograph of narrow leucocratic portion in orthopyroxene granulite. Opx: orthopyroxene, Qtz: quartz, Pl: plagioclase, Mpt: mesoperthite. (c) BSE images of mesoperthite 03D-G1 ((c)-1) and 03D-G2 ((c)-2). Light areas are Or-lamellae and dark ones are Pl-lamellae. Average compositions of Or-lamellae and Pl-lamellae are listed in Table 1.

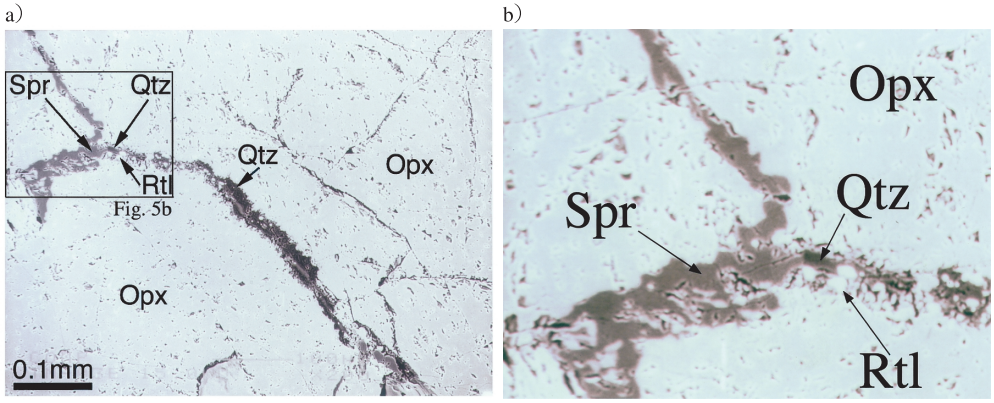

Fig. 5. (a) Back scattered electron (BSE) image of sapphirine coexisting with quartz at the grain boundary of granoblastic orthopyroxene. Scale is 0.1 mm. Opx: orthopyroxene, Spr: sapphirine, Qtz: quartz, Rtl: rutile. (b) Expanded BSE image of area marked in Fig. 5a.

determine H_2O (+).

In metamorphosed ultramafic rock (TM981229-03C), olivine is Fo90–92. Brown

spinel is chromian: $Cr/(Al+Cr)=0.3$–0.5. Serpentine $Mg/(Mg+Fe_{total})=0.93$–0.97. In phlogopite-bearing pyroxene granulite (TM981229-03E), greenish spinel is ferrous with 0.6 Mg atoms per 4 oxygens and $Cr/(Al+Cr)=0.04$–0.05. Sapphirine $Mg/(Mg+Fe_{total})=0.82$–0.84. Chemical compositions of other major minerals are described below.

3.1. Alkali feldspar

Alkali feldspar in orthopyroxene felsic gneiss and pyroxene granulite is perthite to mesoperthite. Sanidine is also found in phlogopite-bearing pyroxene granulite. Average compositions of orthoclase (Or) and plagioclase (Pl) lamellae for mesoperthite in

Table 2. Average compositions of Or and Pl lamellae in mesoperthite and plagioclase porphyroblasts from TM981229-03B and 03D.

	TM981229-03B							
	03B-G1		03B-G2		03B-G3		03B-G4	
	Or lamella (48%)		Or lamella (53%)		Or lamella (58%)		Or lamella (61%)	
	Mean(5)	Std.Dev.	Mean(5)	Std.Dev.	Mean(5)	Std.Dev.	Mean(5)	Std.Dev
wt%								
SiO_2	63.79	0.63	63.68	0.22	63.44	0.50	63.48	0.46
Al_2O_3	18.98	0.29	19.01	0.23	18.89	0.26	18.82	0.14
CaO	0.14	0.08	0.23	0.18	0.18	0.16	0.14	0.04
BaO	0.97	0.13	0.80	0.08	0.89	0.10	0.91	0.09
Na_2O	1.78	0.22	2.01	0.28	2.05	0.14	2.09	0.12
K_2O	14.73	0.32	14.46	0.47	14.09	0.30	14.31	0.26
Total	100.39		100.19		99.54		99.76	
Cations	(O=8)		(O=8)		(O=8)		(O=8)	
Si	2.953	0.004	2.948	0.007	2.954	0.005	2.954	0.007
Al	1.036	0.005	1.038	0.007	1.037	0.008	1.032	0.006
Ca	0.007	0.004	0.011	0.009	0.009	0.008	0.007	0.002
Ba	0.018	0.002	0.015	0.002	0.016	0.002	0.017	0.002
Na	0.160	0.021	0.180	0.024	0.185	0.012	0.189	0.012
K	0.870	0.015	0.855	0.030	0.837	0.024	0.850	0.013
Total	5.044		5.049		5.038		5.049	
	Pl lamella (52%)		Pl lamella (47%)		Pl lamella (42%)		Pl lamella (39%)	
	Mean(4)	Std.Dev.	Mean(4)	Std.Dev.	Mean(5)	Std.Dev.	Mean(5)	Std.Dev.
wt%								
SiO_2	57.89	0.14	57.61	0.94	58.26	0.49	57.41	0.34
Al_2O_3	26.30	0.51	26.05	0.60	26.16	0.49	26.31	0.38
CaO	7.96	0.30	7.81	0.37	7.81	0.33	8.10	0.16
BaO	0.10	0.07	0.06	0.06	0.10	0.10	0.08	0.07
Na_2O	7.60	0.11	7.51	0.24	7.55	0.09	7.41	0.19
K_2O	0.28	0.28	0.26	0.24	0.47	0.36	0.18	0.10
Total	100.14		99.31		100.35		99.51	
Cations	(O=8)		(O=8)		(O=8)		(O=8)	
Si	2.591	0.016	2.602	0.010	2.607	0.013	2.590	0.010
Al	1.387	0.017	1.387	0.009	1.380	0.016	1.399	0.013
Ca	0.382	0.012	0.378	0.014	0.374	0.013	0.391	0.007
Ba	0.002	0.001	0.001	0.001	0.002	0.002	0.001	0.001
Na	0.660	0.006	0.658	0.012	0.655	0.009	0.648	0.014
K	0.016	0.016	0.015	0.014	0.027	0.021	0.011	0.006
Total	5.038		5.041		5.045		5.040	

the matrix of felsic gneiss (TM981229-03Bf) and in the leucocratic portion of phlogopite-free pyroxene granulite (TM981229-03D: Fig. 4) are given in Table 2. Compositions of the Pl lamellae are An34–40 in orthopyroxene felsic gneiss and An41–43 in the leucocratic portion of pyroxene granulite. Anorthite contents are equal to or less than those of coexisting plagioclase (An41–60 and An40–50, respectively) (Fig. 6). Compositions of Or lamellae in the same mesoperthite grains are Or80–89 with 0.74–1.12 wt% BaO in orthopyroxene felsic gneiss and Or85–89 with 1.36–2.09 wt% BaO in leucocratic portion of the pyroxene granulite. Sanidine has 0.78 wt% BaO. Original compositions of feldspar restored from the Or and Pl lamellae in mesoperthite by the method of Yoshimura *et al.* (2000) are presented in Fig. 6. The restored compositions

Table 2. (Continued).

	TM981229-03D 03D-G1 Or lamella (46%)		03D-G2 Or lamella (46%)		TM981229-03B Plagioclase -Porphyroblast		TM981229-03D Plagioclase -Porphyroblast	
	Mean(26)	Std.Dev.	Mean(28)	Std.Dev.	Mean(21)	Std.Dev.	Mean(13)	Std.Dev.
wt%								
SiO_2	63.04	0.67	63.34	0.38	55.83	1.31	57.18	0.57
Al_2O_3	18.83	0.19	18.80	0.12	27.78	0.69	26.55	0.56
CaO	0.09	0.05	0.10	0.06	9.70	0.77	8.84	0.59
BaO	1.69	0.10	1.51	0.14	0.07	0.07	0.06	0.05
Na_2O	1.39	0.10	1.38	0.10	6.62	0.48	6.54	0.27
K_2O	14.66	0.24	14.71	0.15	0.11	0.05	0.12	0.05
Total	99.70		99.85		100.11		99.29	
Cations	(O=8)		(O=8)		(O=8)		(O=8)	
Si	2.952	0.010	2.958	0.004	2.511	0.040	2.578	0.027
Al	1.039	0.010	1.034	0.005	1.473	0.040	1.410	0.026
Ca	0.004	0.002	0.005	0.003	0.468	0.040	0.427	0.027
Ba	0.031	0.002	0.028	0.003	0.001	0.001	0.001	0.001
Na	0.126	0.009	0.125	0.009	0.577	0.038	0.572	0.024
K	0.876	0.017	0.877	0.008	0.006	0.003	0.007	0.003
Total	5.029		5.026		5.036		4.995	

	Pl lamella (54%)		Pl lamella (54%)	
	Mean(26)	Std.Dev.	Mean(28)	Std.Dev.
wt%				
SiO_2	57.10	0.62	57.13	0.32
Al_2O_3	26.35	0.27	26.45	0.26
CaO	8.63	0.12	8.76	0.14
BaO	0.09	0.07	0.03	0.03
Na_2O	6.72	0.14	6.64	0.09
K_2O	0.16	0.07	0.12	0.03
Total	99.04		99.14	
Cations	(O=8)		(O=8)	
Si	2.585	0.012	2.583	0.009
Al	1.407	0.015	1.409	0.009
Ca	0.419	0.007	0.425	0.006
Ba	0.002	0.001	0.001	0.001
Na	0.590	0.011	0.582	0.006
K	0.009	0.004	0.007	0.002
Total	5.011		5.007	

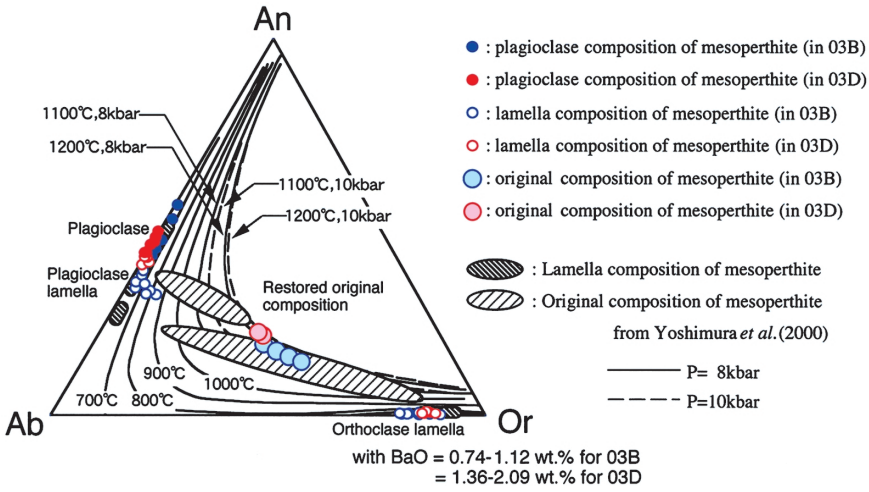

Fig. 6. An-Ab-Or ternary feldspar diagram for original feldspar compositions restored from plagioclase and orthoclase lamellae in mesoperthite from matrix of orthopyroxene felsic gneiss and leucocratic domain of orthopyroxene granulite. Ternary miscibility gaps are traced from Yoshimura et al. (2000), calculated using the method of Kroll et al. (1993).

are on the 1200°C isotherm at 8–10 kbar for the An-Ab-Or ternary feldspar system.

3.2. *Orthopyroxene*

Compositional variation of orthopyroxene in metamorphosed ultramafic rock and associated rocks are given in Fig. 7. Aluminum content in orthopyroxene grains decrease from core to rim for all rock samples. The $Mg/(Mg+Fe_{total})$ values of orthopyroxene in metamorphosed ultramafic rocks are the highest (0.90–0.92) and those

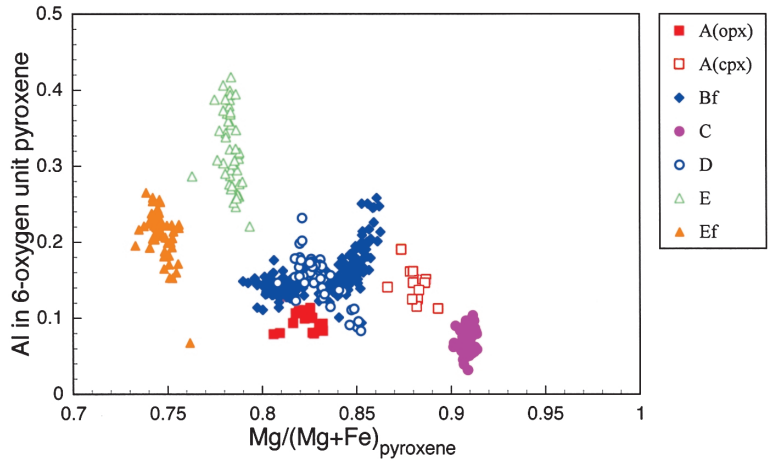

Fig. 7. Variations in Al content (per 6-oxygen formula unit) and $Mg/(Mg+Fe_{total})$ of orthopyroxene in metamorphosed ultramafic rock and associated rocks.

in felsic gneiss are the lowest (0.73–0.76) amongst the metamorphosed ultramafic rock and associated rocks. Aluminum content of orthopyroxene in metamorphosed ultramafic rocks is the lowest (0.03–0.10 Al atoms per 6 oxygens). Orthopyroxene in phlogopite-bearing pyroxene granulites (TM981229-03E) has the most aluminous composition (5.3 to 9.9 wt% of Al_2O_3, corresponding to 0.22–0.42 Al atoms per 6 oxygens). In an orthopyroxene felsic gneiss (TM981229-03Bf) which bordering pyroxene granulite, $Mg/(Mg+Fe_{total})$ values and Al contents of orthopyroxene decrease away from the contact with pyroxene granulite. In a pyroxene granulite (TM981229-03D) with a narrow leucocratic portion (Fig. 4), on the other hand, $Mg/(Mg+Fe_{total})$ values increase and Al content decreases away from the contact.

Table 3. Average compositions of phlogopite from TM981229-03A, 03C and 03E.

	TM981229-03A		TM981229-03C		TM981229-03E	
	Mean(3)	Std.Dev.	Mean(70)	Std.Dev.	Mean(4)	Std.Dev.
wt.%						
SiO_2	40.39	1.10	42.10	0.42	40.04	0.33
TiO_2	3.36	0.40	0.48	0.07	5.55	0.36
Al_2O_3	14.64	0.37	13.16	0.31	13.29	0.11
Cr_2O_3	0.51	0.34	0.38	0.10	0.27	0.03
FeO	5.27	0.15	1.38	0.13	5.98	0.20
MnO	0.01	0.01	0.04	0.04	0.02	0.02
MgO	21.51	0.79	26.33	0.34	20.20	0.42
Na_2O	0.00	0.00	0.64	0.08	0.55	0.05
K_2O	9.95	0.15	10.77	0.17	10.44	0.47
Total (Cation)	95.64		95.28		96.34	
$H_2O(+)$*1					0.54	
$H_2O(-)$*1					0.06	
F*2					4.05	
Total (Anion)					4.60	
Cations	(O=22)		(O=22)		(O=22)	
Si	5.714	0.048	5.916	0.032	5.699	0.026
Ti	0.358	0.046	0.051	0.008	0.595	0.039
Al	2.442	0.043	2.180	0.044	2.229	0.026
Cr	0.057	0.038	0.042	0.011	0.030	0.003
Fe	0.624	0.026	0.162	0.016	0.712	0.027
Mn	0.001	0.001	0.005	0.005	0.002	0.002
Mg	4.536	0.075	5.515	0.044	4.286	0.071
Na	0.000	0.000	0.174	0.020	0.152	0.013
K	1.797	0.057	1.932	0.026	1.895	0.011
Total Cations	15.578		15.977		15.600	
OH(+)*1					0.513	
OH(-)*1					0.057	
F*2					1.823	
Total Anions					2.393	

*1: $H_2O(+)$ and $H_2O(-)$ contents of phlogopite separated from phlogopite-bearing orthopyroxene granulite (TM981229-03E), determined by Karl-Fischer method (Muroi, 1979).
*2: Fluorine content was determined by JEOL Model JXA-8800 Superprobe at Ehime University. Original data was presented in Sato *et al.* (2002).

3.3. Phlogopite

Colorless phlogopite in metamorphosed ultramafic rock (TM981229-03C) is highly magnesian ($Mg/(Mg+Fe_{total})=0.96$–0.98), with 5.4 to 5.7 Mg atoms and 2.0 to 2.3 Al atoms per 22 oxygens (Table 3). It contains 0.35–0.62 wt% of TiO_2. Brown phlogopite in clinopyroxene-bearing pyroxene granulite (TM981229-03A) is magnesian ($Mg/(Mg+Fe_{total})=0.87$–0.88), with 4.5 to 4.6 Mg atoms and 2.4 to 2.5 Al atoms per 22 oxygens. It contains 3.09–3.82 wt% of TiO_2. Brown phlogopite in another pyroxene granulite (TM981229-03E) is also magnesian ($Mg/(Mg+Fe_{total})=0.85$–0.86), with 4.2 to 4.4 Mg atoms and 2.2 to 2.3 Al atoms per 22 oxygens. It contains 5.02–5.81 wt% of TiO_2. It has abundant fluorine (nearly 4 wt%: Sato *et al*., 2002) and is poor in H_2O ($H_2O(-)=0.06$ wt%, $H_2O(+)=0.54$ wt%) (Table 3).

4. Whole rock chemistry

Major chemical compositions of whole rock samples were determined by X-ray fluorescence spectrometry (XRF: Rigaku-GF06P) at Kyushu University following calibration techniques using glass discs (Nakada *et al*., 1985). The same rock samples were analyzed for minor element compositions (Sc, V, Cr, Ni, Cu, Zn, Y, Zr, Nb, Ba, La and Ce) by inductively coupled plasma atomic emission spectrometry (ICP-AES: Seiko Instruments, SPS-1200AR) after decomposition by HF and NHO_3 and conditioning by dilute HCl. Rubidium, strontium, samarium and neodymium concentrations were determined by conventional isotope dilution methods at the same time of isotope analysis. Water ($H_2O(+)$ and $H_2O(-)$) contents of the metamorphic rock samples were determined by the Karl-Fischer method.

Analytical results of major and minor compositions for metamorphosed ultramafic rock and associated rocks are given in Table 4. Metamorphosed ultramafic rock and pyroxene granulites have high contents of LIL elements such as Rb and Ba in spite of their mafic compositions with plentiful compatible elements such as Ni, Cr and MgO. Orthopyroxene felsic gneiss and pyroxene granulite, beside phlogopite-bearing pyroxene granulite, are poor in H_2O. Metamorphosed ultramafic rock contains only a little H_2O, reflecting the presence of serpentine. Zinc content of the metamorphosed ultramafic rock is lower than that of pyroxene granulites, though Zn is expected to show the same behavior as Mg due to the same coordination numbers and similar ion radii (Taure *et al*., 1998). Yttrium contents of pyroxene granulites are higher than those of metamorphosed ultramafic rock and orthopyroxene felsic gneiss (Fig. 8a). LREE (La, Ce, Nd and Sm) contents of pyroxene granulite are equivalent to or more than those of orthopyroxene felsic gneisses. LREE and Y abundances of the pyroxene granulites and orthopyroxene felsic gneisses normalized to CI chondrite composition (McDonough and Sun, 1995) are given in Fig. 8b. The normalized values for LREE concentrations decrease from La to Sm. Normalized values for Y, which behaves as a HREE due to its similar ion radius to Ho in the 3+ oxidation state, are slightly lower than those of LREE.

Table 1. Major and minor element compositions of metamorphosed ultramafic rock (*-C), pyroxene granulite (*-A, *-D, *-E), and felsic gneiss (*-Ef, *-F) from Howard Hills.

TM981229-	03A	03C	03D	03E	03Ef	03F
(wt%)						
SiO_2	52.83	43.62	53.10	46.91	76.14	72.36
TiO_2	0.23	0.07	0.14	1.57	0.15	0.02
Al_2O_3	5.18	1.33	4.91	13.48	11.61	14.04
FeO*	9.45	11.61	9.78	10.39	1.34	1.05
MnO	0.17	0.14	0.20	0.16	0.02	0.06
MgO	29.40	40.56	29.53	21.99	2.54	2.79
CaO	1.12	0.31	0.72	0.59	2.65	2.60
Na_2O	0.17	0.00	0.40	0.31	2.89	2.83
K_2O	0.77	0.31	0.17	2.28	1.48	3.44
P_2O_5	0.02	0.00	0.01	0.09	0.00	0.00
$H_2O(-)$	0.12	0.24	0.17	0.12	0.12	0.17
$H_2O(+)$	0.36	2.13	0.25	0.25	0.20	0.16
Total	99.82	100.01	99.38	98.14	99.14	99.52
(ppm)						
Sc	10.5	10.8	8.4	13.5	21.3	5.0
V	44.8	68.1	30.3	216	4.8	3.7
Cr	930	2171	1176	1827	8.2	1.1
Ni	1359	2834	1291	740	55.2	92.0
Cu	2.8	189	1.3	2.1	0.5	0.4
Zn	112	72.4	127	155	20.0	20.7
Rb	28.6	15.8	8.32	324	32.8	44.9
Sr	11.1	9.77	14.1	29.8	191	159
Y	34.6	0.5	20.8	3.4	0.8	0.4
Zr	85.2	28.5	60.4	123	233	119
Nb	20.2	24.9	17.9	71.4	11.4	7.76
Ba	215	54.7	78.8	1073	721	2230
La	53.5	u.d.	11.0	16.8	57.8	45.1
Ce	98.2	u.d.	18.7	24.8	82.9	55.4
Nd	20.0	0.757	0.907	6.89	22.0	11.83
Sm	4.44	0.222	0.246	1.33	2.45	1.042
$^{87}Rb/^{86}Sr$	7.693	4.793	1.722	35.72	0.4994	0.8233
$^{87}Sr/^{86}Sr$	1.02456(23)	0.92614(8)	0.80025(15)	2.09460(17)	0.75408(28)	0.76440(9)
$^{147}Sm/^{144}Nd$	0.1341	0.1774	0.1642	0.1165	0.06724	0.05323
$^{143}Nd/^{144}Nd$	0.51095(7)	0.51170(8)	0.51141(5)	0.51058(5)	0.50976(9)	0.50950(6)
-C.I.P.W.Norm-						
quartz	0.00	0.00	0.00	0.00	46.40	32.11
orthoclase	4.52	1.55	0.63	14.58	8.72	20.30
albite	0.99	1.03	2.84	4.66	21.73	23.95
anorthite	5.40	1.44	3.42	2.44	12.81	12.88
corundum	2.58	0.66	3.45	9.32	1.22	0.94
hyperthene	77.74	13.89	74.02	45.52	7.76	8.97
olivine	7.54	83.15	17.31	20.38	0.00	0.00
ilmenite	0.41	0.07	0.21	3.24	0.24	0.03
apatite	0.11	0.00	0.04	0.44	0.06	0.02

03E and 03Ef; Phlogopite-bearing Opx granulite and Opx bearing felsic gneiss of TM981229-03E.
Major elements were determined by X-ray fluorescence spectrometry (Rigaku-GF3063P). Total iron as FeO. $H_2O(+)$ and $H_2O(-)$ contents of them were determined by Karl-Fischer method under an N_2 atmosphere, the temperature was increased up to 120°C to determine the $H_2O(-)$ and then to 980°C to determine the $H_2O(+)$. Minor elements (except Rb, Sr, Sm and Nd) were determined by Inductively Coupled Plasma atomic Emission Spectrometry (Seiko Instruments SPS1200AR). Rubidium contents were analyzed by HITACHI RMU5G mass spectrometer. Strontium, samarium and neodymium were analyzed by JEOL JMS05RB mass spectrometer. Errors for isotope ratios in parentheses given are $\pm 1\sigma$.

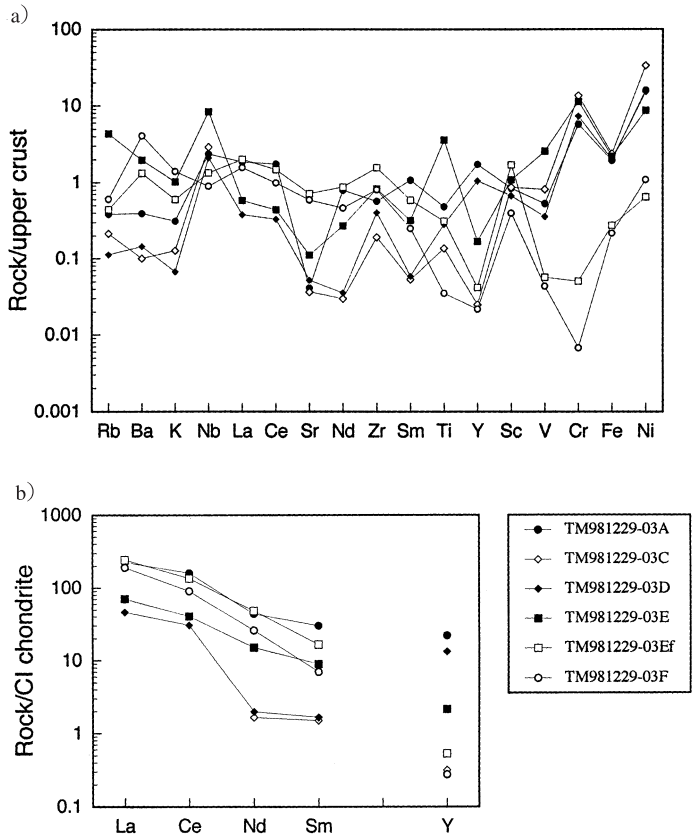

Fig. 8. (a) Trace element concentrations normalized to the average chemical composition of juvenile upper continental crust in the Late Archean (Condie, 1993). (b) LREE (La, Ce, Nd and Sm) and Y concentrations normalized to the composition of CI chondrite (McDonough and Sun, 1995). Some trace element compositions of pyroxene granulite (filled symbols) lie beyond the ranges between metamorphosed ultramafic rock and orthopyroxene felsic gneiss (open symbols).

5. Isotope chemistry

Conventional isotope dilution methods were applied to determine Rb, Sr, Sm and Nd compositions of the rock samples. Decomposed sample fractions were resolved with HCl-$(COOH)_2$ mixed acid, and then passed through the cation exchange resin DOWEX 50W-X8, 200 mesh to separate Rb, Sr and REE fractions. Samarium and neodymium were separated from the REE fraction by passing through another cation exchange resin adjusted with ammonia, following the separation method of Kubota (1992). Rubidium concentration was determined with a HITACHI RMU5G mass spectrometer. Strontium and neodymium isotope composition and total Sr, Sm and Nd concentrations were determined with JEOL JMS05RB mass spectrometer. The strontium standard of Eimer and Amend gave values of $^{87}Sr/^{86}Sr = 0.7080 \pm 0.0001$ (1σ) and

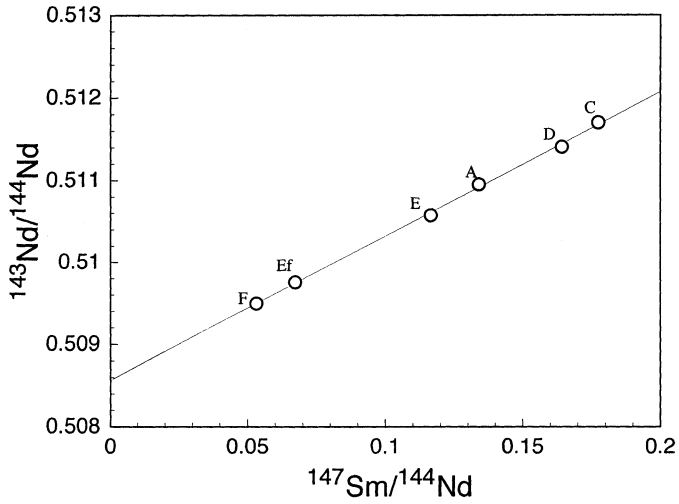

Fig. 9. Sm-Nd isochron diagram for whole rock samples. Letters identifying points refer to sample numbers. Samarium and neodymium isotope compositions of six bulk rock samples form a linear array on the isochron diagram. The line defined by least square regression method (York, 1966), has a slope with an apparent age of 2.66±0.05 Ga, and an intercept at $^{143}Nd/^{144}Nd = 0.50856 \pm 0.00004$ ($\varepsilon_{Nd,CHUR}^{isochron,2.66Ga} = -12.3 \pm 0.9$) (errors are ±1σ).

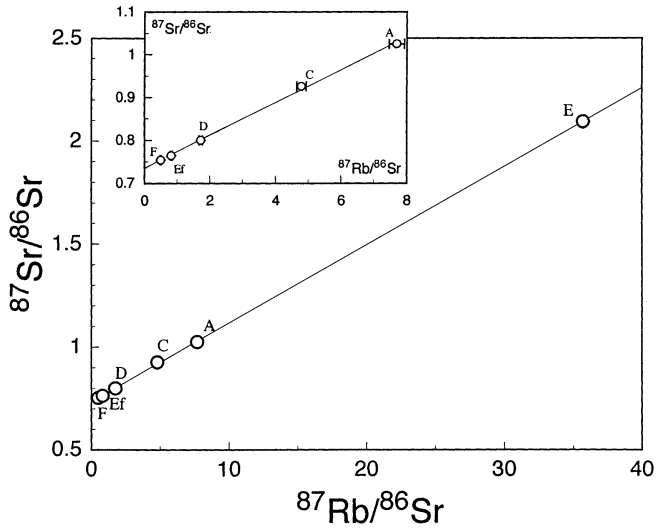

Fig. 10. Rb-Sr isochron diagram for whole rock samples. Letters identifying points refer to sample numbers. Rubidium and strontium compositions of the bulk rock samples form a linear array on the isochron diagram. The line defined by least square regression method (York, 1966), has a slope with an apparent age of 2.63±0.03 Ga, and an intercept at $^{87}Sr/^{86}Sr = 0.7357 \pm 0.0024$ (errors are ±1σ).

NBS983 gave values of $^{87}Sr/^{86}Sr = 0.7103 \pm 0.0001$ (1σ) in this study. The neodymium standard of JNdi-1 (GSJ standard) gave the values of $^{143}Nd/^{144}Nd = 0.51212 \pm 0.00004$ (1σ) in this study. Relative analytical errors in Rb, Sr, Sm and Nd concentrations are 2%, 1%, 0.5% and 1%, respectively. The contamination levels of Rb, Sr, Sm and Nd are 1×10^{-10}g, 3×10^{-10}g, 1×10^{-10}g and 1×10^{-10}g per sample. The decay constants for ^{87}Rb and ^{147}Sm used are 1.42×10^{-11}year^{-1} (Steiger and Jäger, 1977) and 6.54×10^{-12}year^{-1} (Lugmair and Marti, 1978). The chondritic uniform reservoir (CHUR) parameters for the calculation of epsilon Nd values at t years ago ($\varepsilon^{t}_{Nd,CHUR}$) and Nd model ages ($T_{CHUR}$) used are $^{143}Nd/^{144}Nd$ (present) = 0.512638 and $^{147}Sm/^{144}Nd$ (present) = 0.1966 (Hamilton *et al*., 1983).

Rb-Sr and Sm-Nd analytical data for whole rock samples are listed in Table 4. Samarium and neodymium isotope compositions of six bulk rock samples form a linear array on the isochron diagram, even though the rock species are different each other. The regressed line has a slope with an apparent age of 2.66 ± 0.05 Ga, and intercept at $^{143}Nd/^{144}Nd = 0.50856 \pm 0.00004$ (Fig. 9). Rubidium and strontium compositions of the bulk rock samples also plot linearly on the isochron diagram. The regressed line has a slope with an apparent age of 2.63 ± 0.03 Ga, and intercept at $^{87}Sr/^{86}Sr = 0.7357 \pm 0.0024$ on the isochron diagram (Fig. 10).

6. Discussion

6.1. Considerations of metamorphic conditions based on petrography of metamorphic rocks

Sapphirine coexists with quartz as thin films along grain boundaries of granoblastic orthopyroxene in phlogopite-rich pyroxene granulite from Howard Hills (TM981229-03E: Fig. 5). This paragenesis provides evidence of ultra-high temperature (UHT) metamorphism (over 1030°C at 9.5 kbar or over 1050°C at 11 kbar; Hensen and Green, 1973; Bertrand *et al*., 1991). Hokada *et al*. (1999) has reported film-like sapphirine at the grain boundaries of granoblastic orthopyroxene in aluminous gneiss of the same occurrences, and interpreted this as products from the breakdown of highly aluminous orthopyroxene at retrograde stage of UHT metamorphism. The metamorphic grade of the granulite from Howard Hills may therefore be higher than *P-T* estimates derived from the coexistence of sapphirine and quartz.

Mesoperthite grains are found in the matrix of orthopyroxene felsic gneiss and in the leucocratic portion within pyroxene granulite (Fig. 4). Original compositions of feldspar restored from the Or and Pl lamellae of mesoperthite indicate equilibrium at 1150–1200°C (Fig. 6). This result coincides with evidence of UHT metamorphism demonstrated from sapphirine-quartz coexistence in pyroxene granulite, and is the same result as geothermometry for restored mesoperthite compositions in felsic gneisses and aluminous gneisses from Howard Hills (Yoshimura *et al*., 2000).

Average BaO content of Or lamellae within mesoperthite range 0.8 to 1.7 wt% in the matrix of orthopyroxene felsic gneiss and in the leucocratic portion in pyroxene granulite (Table 2). Plagioclase coexisting with mesoperthite contains over 40 mol% An in average, and up to 50 mol%. Yoshimura *et al*. (2000) suggested the possibility of partial melting during metamorphism from zoning of garnet with abundant Y and

HREE, high BaO content in Or lamella of mesoperthite (up to 2.7 wt%), and high An content in plagioclase (up to 80 mol%) in felsic gneiss. The BaO content of Or lamella or An content of plagioclase from orthopyroxene felsic gneiss and pyroxene granulite are also elevated considering the felsic composition of the host, although they are not so high as those in garnet felsic gneiss from Howard Hills (Yoshimura *et al*., 2000). Pyroxene granulite associated with leucocratic portions were probably influenced by partial melting or segregated melt from a common protolith.

Under UHT metamorphic conditions, breakdown of biotite provides H_2O-fluid and/or controls fluid-absent melting (Bohlen *et al*., 1983; Vielzeuf and Clemens, 1992). The stability field of fluorine-rich phlogopite extends to higher temperatures than that of fluorine-poor phlogopite (Motoyoshi and Hensen, 2001). However, decomposition of F-rich phlogopite (3.6 wt% fluorine) coexisting with quartz generates felsic melt with orthopyroxene residue at over 1100°C (Tareen *et al*., 1995). Coexistence of phlogopite and quartz have not been observed in pyroxene granulites from Howard Hills, although phlogopite-bearing pyroxene granulite contains rare quartz with sapphirine as isolated thin films along grain boundaries of granoblastic orthopyroxene. Synthetic experiments with glass made from pyroxene granulite with seed mineral aggregate yield felsic melt under UHT metamorphic conditions (Sato *et al*., 2003, 2004). The pyroxene granulites are probably residual after incongruent melting of phlogopite-rich protoliths during UHT metamorphism.

Metamorphosed ultramafic rock (TM981229-03C) contains minor amount of serpentine. This appearance is an evidence of hydrothermal event with temperatures lower than 650°C (Wunder and Schreyer, 1997) after UHT metamorphism. However, there is no evidence of the hydrothermal event in pyroxene granulite nor in felsic gneiss. Therefore, hydrothermal activity was minor and its effect is restricted to metamorphosed ultramafic rock.

6.2. Possibility of homogenization of isotopic compositions during the metamorphism

Whole rock samples of metamorphosed ultramafic rock, pyroxene granulite and felsic gneiss from the Howard Hills have varied compositions. Although it is not expected that different rock types would have the same initial $^{87}Sr/^{86}Sr$ and $^{143}Nd/^{144}Nd$ ratios, their Rb-Sr and Sm-Nd isotope ratios form linear arrays on isochron diagrams (Figs. 9 and 10). This fact should be considered before interpreting apparent ages estimated from the linear arrangement of isotope ratios. In particular, alteration of bulk compositions must not be ignored for metamorphic rocks, considering the possibility of mass transportation by partial melting during prograde metamorphism.

Mingling of two components with different Rb/Sr and $^{87}Sr/^{86}Sr$ ratios will produce a straight line connecting the endmembers on an isochron diagram (fictitious isochron: Faure, 1986). When two components with different Rb/Sr and $^{87}Sr/^{86}Sr$ ratios mix with each other, the $^{87}Sr/^{86}Sr$ ratio and Sr concentrations of mixtures are related by a hyperbolic equation that transforms into a line by inverting the Sr concentrations (Faure, 1986). However, the $^{87}Sr/^{86}Sr$ ratios and the reciprocals of the Sr concentrations of the metamorphic rocks from Howard Hills do not form a linear array, except for estimated Sr compositions before 2.63 b.y. (solid line on Fig. 11a), which is an apparent age calculated from a line on isochron diagram (Fig. 10). We conclude that the linear

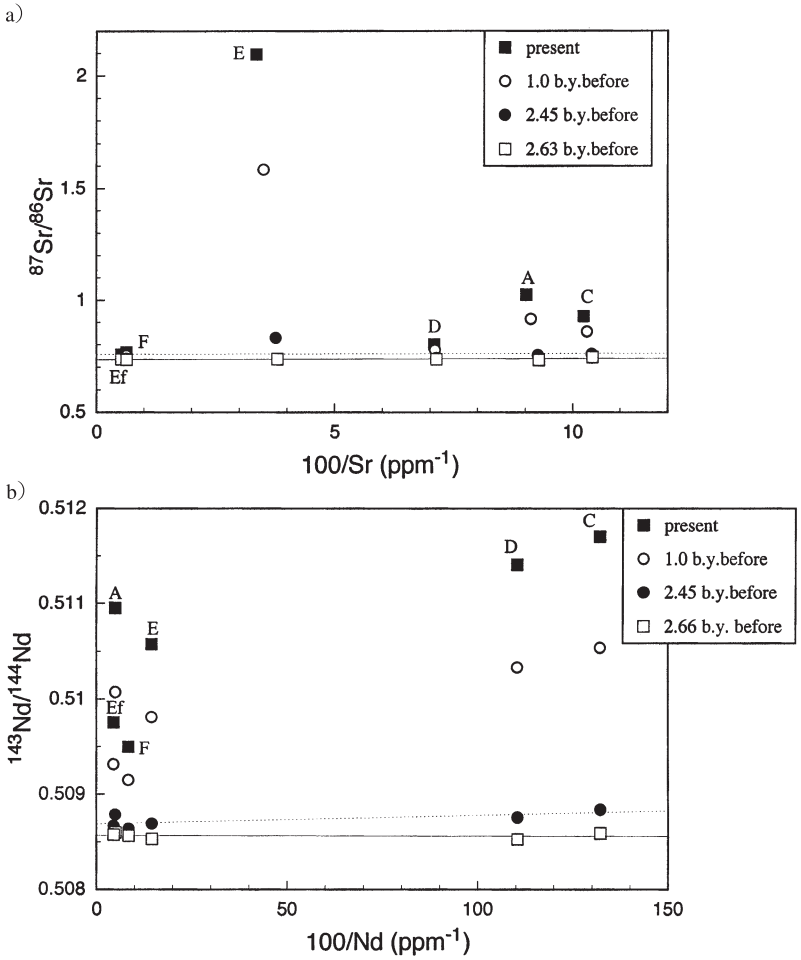

Fig. 11. (a) Plots of $^{87}Sr/^{86}Sr$ ratios and reciprocals of Sr concentrations of metamorphosed ultramafic rock and associated rocks. Solid line shows regression for $^{87}Sr/^{86}Sr$ values at 2.63 billion years ago, which is an apparent age calculated from the isochron diagram (Fig. 10), and a dotted line shows regression for $^{87}Sr/^{86}Sr$ at 2.45 billion years ago, which is the U-Pb and Pb-Pb concordant age of zircon in felsic gneiss from Howard Hills (Miyamoto et al., 2003). (b) Plots of $^{143}Nd/^{144}Nd$ ratios and the reciprocals of the Nd concentrations of the metamorphosed ultramafic rock and associated rocks. A solid line shows regression for $^{143}Nd/^{144}Nd$ values at 2.66 billion years ago, which is an apparent age calculated from the isochron diagram (Fig. 9), and a dotted line shows regression for $^{143}Nd/^{144}Nd$ at 2.45 billion years ago.

array of Rb and Sr compositions of the bulk rock samples do not represent a fictitious isochron derived from the mixing of ultramafic and felsic endmembers. On a diagram of $^{143}Nd/^{144}Nd$ ratios and the reciprocals of the Nd concentrations, Nd compositions of the metamorphic rocks from Howard Hills do not form a linear array, except for estimated Nd compositions before 2.66 b.y. (solid line on Fig. 11b), which is an

apparent age calculated from linear arrangement on an isochron diagram (Fig. 9), even though analytical errors of Nd isotope ratio are large. Strontium and neodymium isotope compositions make it clear that compositions of pyroxene granulites cannot be explained by mixing of metamorphosed ultramafic rock and orthopyroxene felsic gneiss during high temperature metamorphism.

Although whole rock compositions of pyroxene granulites are approximately intermediate between inner metamorphosed ultramafic rock and outer orthopyroxene felsic gneiss (*e.g*., MgO, Cr, Ni, in Table 4), some major and trace element compositions of pyroxene granulites in which Ti, Y and REE are regarded as immobile elements during hydrothermal activity, are out of the compositional range between the ultramafic and felsic rocks (Fig. 8). This occurrence is also evidence that pyroxene granulite compositions do not represent a mixture of the ultramafic and felsic endmembers. Among these elements, Rb, Ti and Nb are abundant in phlogopite-bearing pyroxene granulite, and Ce and Sm are enriched in clinopyroxene-bearing pyroxene granulite. Rubidium and titanium are major constituent elements of phlogopite and Nb is also compatible. Yttrium, cerium and samarium are distributed between phlogopite, orthopyroxene, and especially clinopyroxene (Rollinson, 1993). Compositional characters of pyroxene granulites might be explained by elemental compatibilities of major constituent minerals formed at metamorphism.

Strontium seems to be mobile during metamorphism, but isotopic homogenization of Sr on a meter scale is unlikely under dry conditions. The REEs are less mobile than alkali metals and alkali earths during regional metamorphism and hydrothermal alteration (Faure, 1986). Efficient isotopic homogenization of Sr and Nd between mafic and felsic rocks can be achieved under granulite-facies metamorphic conditions by fluid and melt migration (Pan *et al*., 1999). Hammouda *et al*. (1996) estimated the time required for Sr isotopic homogenization between melt and residue at 10^4 to 10^6 years for temperatures ranging from 800 to 1000°C and grain sizes 1 to 10 mm, from the Sr isotope profile of run products by synthetic experiments on partial melting of plagioclase and F-phlogopite assemblages. The possibility of partial melting during metamorphism was suggested from occurrences of metamorphic rocks in previous discussions. Isotopic homogenization of Sr and Nd by melt generated during metamorphism is feasible for metamorphosed ultramafic rock and associated rocks from Howard Hills. The coincidence of apparent Rb-Sr and Sm-Nd ages (Figs. 9 and 10) probably indicates that Sr and Nd isotope ratios were homogenized among metamorphosed ultramafic rock and associating rocks during UHT metamorphism, at about 2.65 Ga.

The Napier Complex is regarded as a granulite facies to UHT metamorphic terrane formed at 2.4–2.5 Ga (*e.g*., Hokada *et al*., 2001; Asami *et al*., 2002; Carson *et al*., 2002), according to the results of many geochronological studies, especially recent SHRIMP dating of zircon and CHIME ages of monazite and zircon grains in the metamorphic rocks, although the possibility of older metamorphic ages was also suggested by Harley and Black (1997), Harley *et al*. (2001), and Crowe *et al*. (2002). Zircon grains with near concordant U-Pb and Pb-Pb ages of 2.45 Ga were found in orthopyroxene felsic gneiss from the Howard Hills (Miyamoto *et al*., 2003). The 0.2 billion year difference between U-Pb age of zircon and Rb-Sr and Sm-Nd whole rock isochron ages should be considered before the apparent ages of 2.65 Ga can be interpreted. One explanation for

the age difference is that following high-grade metamorphism, zircon crystals released radiogenic Pb at 2.45 Ga without participation of melt after UHT metamorphism at 2.65 Ga. Estimated temperatures for the episode might represent the closure temperature of Pb diffusion in zircon (*e.g.*, over 900°C at 10°C/Myr cooling condition, or lower temperatures at slower cooling rates; Cherniak and Watson, 2000), though the concept of closure temperatures has to be applied with utmost care (Kühn *et al.*, 2000). In this case, U-Pb compositions of zircon tend to be discordant, possibly due to incomplete Pb-loss. The deviation of U-Pb composition from the concordia, however, is small over a 0.2 b.y. age interval, and discordant U-Pb compositions would still fall within error of concordia. Another explanation is that granulite-facies metamorphism was maintained with a very low cooling rate after 2.65 Ga. In this case, radiogenic lead in zircon may be released efficiently by diffusion at high temperature (Cherniak and Watson, 2000). Though we have no definite information on the 0.2 billion year difference between the U-Pb age of zircon and Rb-Sr and Sm-Nd whole rock isochron ages, at least, rejuvenation of zircon could be achieved by thermal activity following UHT metamorphism at 2.65 Ga.

The possibility of compositional modification during UHT metamorphism is also strongly supported by estimation of Nd model ages for the metamorphic rocks. Neodymium model ages (T_{CHUR}) are estimated to be 3.37 and 3.31 Ga for orthopyroxene felsic gneiss (TM981229-03Ef and F), and 4.07 and 3.89 Ga for two samples of pyroxene granulite (TM981229-03A and E) (Fig. 12). These estimates are not unreasonable, since some chronological evidence of 3.3 to 4.0 Ga igneous activity has been reported for metamorphic rocks of Napier Complex (DePaolo *et al.*, 1982; Black *et al.*, 1986; Owada *et al.*, 1994; Harley and Black, 1997; Hokada *et al.*, 2003). However, T_{CHUR} for metamorphosed ultramafic rock (TM981229-03C) and phlogopite-free pyroxene

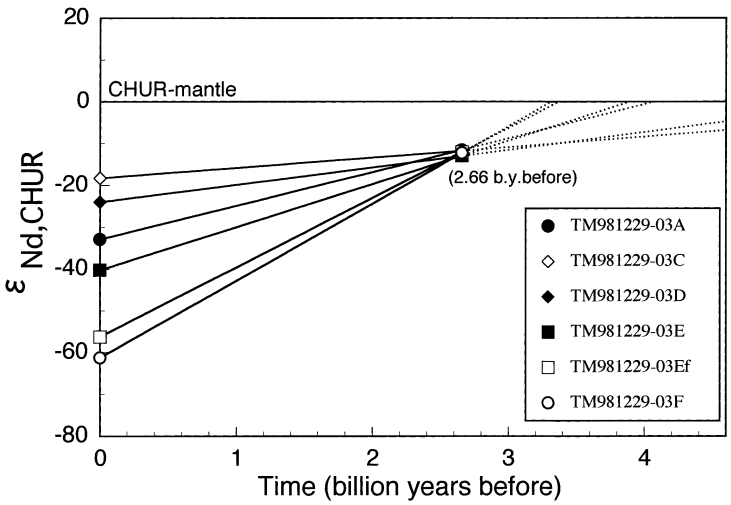

Fig. 12. Plot of $\varepsilon_{Nd,CHUR}$ values against time for metamorphosed ultramafic and associated rocks. Solid lines show evolutions of $\varepsilon_{Nd,CHUR}$ values for rock samples back to 2.66 billion years ago, and dotted lines show apparent estimations of $\varepsilon_{Nd,CHUR}$ values before 2.66 billion years ago.

granulite (TM981229-03D) are estimated at 7.28 and 5.70 Ga, respectively. These older ages are improbable for Earth's crustal rocks. Depleted mantle model ages (T_{DM}) should be older than T_{CHUR}. Therefore, we conclude that the metamorphic rocks have experienced major modification of their whole rock compositions after depletion of source materials from the mantle, and metamorphosed ultramafic rock and pyroxene granulites gained compatible elements and/or lost incompatible elements from the enriched protolith. Considering the petrography of the metamorphic rocks, we should recognize partial melting as the most probable cause of elemental depletion. Pyroxene granulites are probably residues after partial melting during UHT metamorphism. Neodymium isotopic compositions showing improbable T_{CHUR} suggests that metamorphosed ultramafic rock was also restitic, although no evidence was found from mineral assemblage or geochemistry. Orthopyroxene felsic gneiss is probably influenced by the generation of melt. Although T_{CHUR} is not used for geochronological research on the crustal evolution of the Napier Complex, it is helpful for confirmation of elemental migrations in the metamorphic rocks of the Howard Hills.

Strontium isotope compositions of metamorphosed ultramafic rock and associated rocks are restored to 0.7357 ± 0.0024 at 2.63 billion years before. These isotope ratios are improbably high for metamorphic rocks with mafic to ultramafic compositions, and could not be produced by magma directly derived from mantle melting (*e.g.*, $(^{87}Sr/^{86}Sr)_{\text{Bulk Earth, 2.63 Ga}} = 0.7015$, $(^{87}Sr/^{86}Sr)_{\text{Depleted mantle, 2.63 Ga}} = 0.7012$; Ben Othman *et al*., 1984). For felsic gneiss, the Sr isotope ratios are also too high to indicate an igneous origin. These restored Sr isotope ratios indicate the influence of melt derived from LILE-enriched protoliths with high Sr isotope ratios, such as granitic rocks or sediments.

7. Conclusions

The Napier Complex, including the Howard Hills, is regarded as a Latest Archean~Earliest Proterozoic metamorphic terrane. Paragenesis and compositions of major constituent minerals in the metamorphic rocks from Howard Hills provide evidence of UHT metamorphism, accompanied by partial melting. Rb-Sr and Sm-Nd isotope data for whole rock samples define contemporaneous isochron ages of 2.65 Ga within analytical error. Isotopic homogenization of Sr and Nd is expected during the metamorphism accompanied by partial melting among the metamorphosed ultramafic rock and associated rocks. This results in the calculation of improbable Nd model ages (T_{CHUR}), due to an increase of Sm/Nd ratios. This can be attributed to an enrichment of compatible elements and/or depletion of incompatible elements. The metamorphic rocks have high initial Sr isotope ratios, indicating the derivation from LILE-enriched protoliths with high Sr isotope ratios. According to mineralogical and geochemical evidence, we conclude that these metamorphic rocks experienced partial melting during UHT metamorphism. Pyroxene granulites were residues after partial melting of granitic or sedimentary protoliths.

Acknowledgments

We express our sincere thanks to the members of JARE-40 and crew of the icebreaker "*Shirase*", especially Prof. K. Shiraishi, Messrs. Y. Ohashi, K. Maki, S. Harigai, T. Takei and Dr. H. Yamauchi, who assisted in helicopter operations. We would like to thank to Profs. E. S. Grew, H. Ishizuka, T. Kawasaki, T. Yanagi, Drs. Y. Osanai, M. Owada, T. Tsunogae and T. Ikeda for their constructive comments and discussions during field survey and preparation of this manuscript. Constructive criticisms of anonymous reviewers and the support of Dr. T. Hokada as an editor are much appreciated. Thanks also go to Dr. K. Yamashita for advice in chemical analyses. Miyamoto's research was supported financially by Grant-in Aid for Encouragement of Young Scientists (No. 09740407) from the Ministry of Education, Science, Sports and Culture, Japan.

References

Asami, M., Suzuki, K. and Grew, E.S. (2002): Chemical Th-U-total Pb dating by electron microprobe analysis of monazite. Xenotime and zircon from the Archean Napier Complex, East Antarctica: evidence for ultra-high-temperature metamorphism at 2400 Ma. Precambrian Res., **114**, 249–275.

Ben Othman, D., Polve, M. and Allègre, C.J. (1984): Nd-Sr isotopic composition of granulites and constraints on the evolution of the lower continental crust. Nature, **307**, 510–515.

Bertrand, P., Ellis, D.J. and Green, D.H. (1991): The stability of sapphirine-quartz and hyperthene-sillimanite-quartz assemblages: an experimental investigation in the system FeO-MgO-Al_2O_3-SiO_2 under H_2O and CO_2 condition. Contrib. Mineral. Petrol., **108**, 55–71.

Black, L.P., Williams, I.S. and Compston, W. (1986): Four zircon ages from one rock: the history of a 3930 Ma-old granulite from Mount Sones, Antarctica. Contrib. Mineral. Petrol., **94**, 427–437.

Bohlen, S.R., Boettcher, A.L., Wall, V.J. and Clemens, J.D. (1983): Stability of phlogopite-quartz and sanidine-quartz: a model for melting in the lower crust. Contrib. Mineral. Petrol., **83**, 270–277.

Carson, C.J., Ague, J.J. and Coath, C.D. (2002): U-Pb geochronology from Tonagh Island, East Antarctica: implications for the timing of ultra-high temperature metamorphism of the Napier Complex. Precambrian Res., **116**, 237–263.

Cherniak, D.J. and Watson, E.B. (2000): Pb diffusion in zircon. Chem. Geol., **172**, 5–24.

Condie, K.C. (1993): Chemical composition and evolution of the upper continental crust: Contrasting results from surface samples and shales. Chem. Geol., **104**, 1–37.

Crowe, W.A., Osanai, Y., Toyoshima, T., Owada, M., Tsunogae, T. and Hokada, T. (2002): SHRIMP geochronology of a mylonite zone in Tonagh Island: characterization of the last high-grade tectonothermal event in the Napier Complex, East Antarctica. Polar Geosci., **15**, 17–36.

DePaolo, D.J., Manton, W.I., Grew, E.S. and Halpern, M. (1982): Sm-Nd, Rb-Sr and U-Th-Pb systematics of granulite facies rocks from Fyfe Hills, Enderby Land, Antarctica. Nature, **298**, 614–618.

Faure, G. (1986): Principles of Isotope Geology, 2nd ed. New York, John Wiley, 589 p.

Hamilton, P.J., O'Nions, R.K., Bridgwater, D. and Nutman, A. (1983): Sm-Nd studies of Archean metasediments and metavolcanics from West Greenland and their implications for the Earth's early history. Earth Planet. Sci. Lett., **62**, 263–272.

Hammouda, T., Pichavant, M. and Chaussidon M. (1996): Isotopic equilibration during partial melting: an experimental test of the behavior of Sr. Earth Planet. Sci. Lett., **144**, 109–121.

Harley, S.L. and Black, L.P. (1997): A revised Archaean chronology for the Napier Complex, Enderby Land, from SHRIMP ion-microprobe studies. Antarct. Sci., **9**, 74–91.

Harley, S.L., Kinny, P.D., Snape, I. and Black, L.P. (2001): Zircon chemistry and the definition of events in Archaean granulite terrains. 4th International Archaean Symposium 2001, Extended Abstracts, ed. by K.F. Cassidy *et al*. AGSO-Geoscience Australia, Record 2001/37, 511–513.

Hensen, B.J. and Green, D.H. (1973): Experimental study of the stability of cordierite and garnet in pelitic compositions at high pressure and temperatures. III. Synthesis of experimental data and geological applications. Contrib. Mineral. Petrol., **38**, 151–166.

Hokada, T., Osanai, Y., Toyoshima, T., Owada, M., Tsunogae, T. and Crowe, W.A. (1999): Petrology and metamorphism of sapphirine-bearing aluminous gneisses from Tonagh Island in the Napier Complex, East Antarctica. Polar Geosci., **12**, 49–70.

Hokada, T., Shiraishi, K., Misawa, K., Yamaguchi, A. and Kaiden, H. (2001): SHRIMP chronology for Late Archaean igneous and metamorphic events of the Napier Complex, East Antarctica. The 21st Symposium on Antarctic Geosciences, Program and Abstracts, 18–19 October 2001. Tokyo, Natl Inst. Polar Res., 17–18.

Hokada, T., Misawa, K., Shiraishi, K. and Suzuki, S. (2003): Mid to late Archaean (3.3–2.5 Ga) tonalitic crustal formation and high-grade metamorphism at Mt. Riiser-Larsen, Napier Comple, East Antarctica. Precambrian Res., **127**, 215–228.

Ishizuka, H., Ishikawa, M., Hokada, T. and Suzuki, S. (1998): Geology of the Mt. Riiser-Larsen area of the Napier Complex, East Antarctica. Polar Geosci., **11**, 154–171.

Kroll, H., Evangelakakis, C. and Voll, G. (1993): Two-feldspar geothermometry: a review and revision for slowly cooled rocks. Contrib. Mineral. Petrol., **114**, 510–518.

Kubota, M. (1992): Sm-Nd model ages of aeolian dusts in Japan and Hawaii and volcanic rocks on the green-stone belt in the Tanzanian Shield. MS Thesis of Department of Geology, Kyushu University, 78 p (in Japanese with English abstract).

Kühn, A., Glodny, J., Iden, K. and Austrheim H. (2000): Retention of Precambrian Rb/Sr phlogopite ages through Caledonian eclogite facies metamorphism, Bergen Arc Complex, W-Norway. Lithos, **51**, 305–330.

Lugmair, G.W. and Marti, K. (1978): Lunar initial $^{143}Nd/^{144}Nd$: differential evolution of the lunar crust and mantle. Earth Planet. Sci. Lett., **39**, 349–357.

McDonough, W.F. and Sun, S.-S. (1995): The composition of the Earth. Chem. Geol., **120**, 223–253.

Miyamoto, T., Yoshimura, Y., Motoyoshi, Y., Sato, K., Grew, E.S., Dunkley, D.J. and Carson, C.J. (2003): Geochronology of phlogopite-bearing granulite from Howard Hills, Enderby Land, East Antarctica. The 23rd Symposium on Antarctic Geosciences, Program and Abstracts, 16–17 October 2003. Tokyo, Natl Inst. Polar Res., 78.

Motoyoshi, Y. (1998): Ultra-high temperature metamorphism of the Napier Complex, East Antarctica: a metamorphic perspective. Jour. Geol. Soc. Jpn., **104**, 794–807 (in Japanese with English abstract).

Motoyoshi, Y. and Hensen, B.J. (2001): F-rich phlogopite stability in ultra-high-temperature metapelites from the Napier Complex, East Antarctica. Am. Mineral., **86**, 1404–1413.

Muroi, K. (1979): Water in analytical chemistry; Determination of water—Karl Fischer method. Bunseki, **50**, 74–82 (in Japanese).

Nakada, S., Yanagi, T., Maeda, S., Fang, D. and Yamaguchi, M. (1985): X-ray fluorescence analysis of major elements in silicate rocks. Sci. Rept. Dept. Geol., Kyushu Univ., **14**, 103–115 (in Japanese with English abstract).

Osanai, Y., Toyoshima, T., Owada, M., Tsunogae, T., Hokada, T. and Crowe, W.A. (1999): Geology of ultrahigh-temperature metamorphic rocks from the Tonagh Island in the Napier Complex, East Antarctica. Polar Geosci., **12**, 1–28.

Owada, M., Osanai, Y. and Kagami, H. (1994): Isotope equilibration age of Sm-Nd whole-rock system in the Napier Complex (Tonagh Island), East Antarctica. Proc. NIPR Symp. Antarct. Geosci., **7**, 122–132.

Owada, M., Osanai, Y., Tsunogae, T., Toyoshima, T., Hokada, T. and Crowe, W.A. (2000): LREE-enriched mafic gneiss and meta-ultramafic rock from Tonagh Island in the Napier Complex, East Antarctica. Polar Geosci., **13**, 86–102.

Pan, Y., Fleet, M.E. and Longstaffe, F.J. (1999): Melt-related metasomatism in mafic granulites of the Quetico subprovince, Ontario: constants from O-Sr-Nd isotopic and fluid inclusions data. Can. J. Earth Sci., **36**, 1449–1462.

Rollinson, H.R. (1993): Using Geochemical Data: Evaluation, Presentation, Interpretation. London, Longman, 352 p.

Sato, K., Miyamoto, T. and Kawasaki, T. (2002): Phase relations of a granulite from Howard Hills in the

Napier Complex, East Antarctica under UHT conditions. Abstracts of the 109th Annual Meeting of the Geological Society of Japan, 308.

Sato, K., Miyamoto, T. and Kawasaki, T. (2003): Experimental constraints of metamorphic pressure and temperature, and phase relations of a phlogopite-bearing granulite from Howard Hills, Napier Complex, East Antarctica. The 23rd Sympsium on Antarctic Geosciences, Program and Abstract, 16–17 October 2003. Tokyo, Natl Inst. Polar Res., 42 (in Japanese).

Sato, K., Miyamoto, T. and Kawasaki, T. (2004): Experimental constraints of metamorphic pressure and temperature, and phase relations of a phlogopite-bearing granulite from Howard Hills, Napier Complex, East Antarctica. J. Mineral. Petrol. Sci., **73** (in press).

Sheraton, J.W., Tingey, R.J., Black, L.P, Offe, L.A. and Ellis, D.J. (1987): Geology of an unusual Precambrian high-grade metamorphic terrane Enderby Land and western Kemp Land, Antarctica. BMR Bull., **223**, 51 p.

Steiger, R.H. and Jäger, E. (1977): Subcommission on geochronology: convention on the use of decay constants in geo- and cosmo-chronology. Earth Planet. Sci. Lett., **36**, 359–362.

Suzuki, S., Hokada, T., Ishikawa, M. and Ishizuka, H. (1999): Geochemical study of granulites from Mt. Riiser-Larsen, Enderby Land, East Antarctica: Implication for protoliths of the Archaean Napier Complex. Polar Geosci., **12**, 101–125.

Tainosho, Y., Kagami, H., Hamamoto, T. and Takahashi, Y. (1997): Preliminary result for the Nd and Sr isotope characteristics of the Archaean gneisses from Mount Pardoe, Napier Complex, East Antarctica. Proc. NIPR Symp. Antarct. Geosci., **10**, 92–101.

Tareen, J.A.K., Keshava Prasad, A.V., Basavalingu, B. and Ganesha, A.V. (1995): The effect of fluorine and titanium on the vapour-absent melting of phlogopite and quartz. Mineral. Mag., **59**, 566–570.

Taure, H., Yurimoto, H., Kurita, K. and Sueno, S. (1998): Pressure dependence on partition coefficients for trace elements between olivine and the coexisting melts. Phys. Chem. Miner., **25**, 469–484.

Vielzeuf, D. and Clemens, J.D. (1992): The fluid-absent melting of phlogopite+quartz: experiments and models. Am. Mineral., **77**, 1206–1222.

Wunder, B. and Schreyer, W. (1997): Antigolite: High-pressure stability in the system MgO-SiO_2-H_2O (MSH). Lithos, **41**, 213–227.

York, D. (1966): Least-squares fitting of a straight line. Can. J. Phys., **44**, 1079–1086.

Yoshimura, Y., Motoyoshi, Y., Grew, E.S., Miyamoto, T., Carson, C.J. and Dunkley, D.J. (2000): Ultrahigh-temperature metamorphic rocks from Howard Hills in the Napier Complex, East Antarctica. Polar Geosci., **13**, 60–85.